Environmental Archaeology: The Journal of Human Palaeoecology

The seasonal mobility of prehistoric gazelle herds in the Azraq Basin, Jordan: modelling alternative strategies using stable isotopes

--Manuscript Draft--

Manuscript Number:	ENV271R1
Full Title:	The seasonal mobility of prehistoric gazelle herds in the Azraq Basin, Jordan: modelling alternative strategies using stable isotopes
Article Type:	Original Research Paper
Keywords:	Southern Levant; Epipalaeolithic; Neolithic; Stable isotopes; Hunting seasonality; Gazelle mobility
Corresponding Author:	Elizabeth Henton Institute of Archaeology UNITED KINGDOM
Corresponding Author Secondary Information:	
Corresponding Author's Institution:	Institute of Archaeology
Corresponding Author's Secondary Institution:	
First Author:	Elizabeth Henton
First Author Secondary Information:	
Order of Authors:	Elizabeth Henton
	Carol Palmer
	Isabelle Ruben
	Louise Martin
	Andrew Garrard
	Matthew Thirlwall
	Anne-Lise Jourdan
Order of Authors Secondary Information:	
Abstract:	The hunting of Gazella subgutturosa was a dominant practice for Epipalaeolithic and early Neolithic hunter-gatherers in the east Jordan steppe. The seasonal mobility of this taxon in the Levant is poorly understood, especially for early prehistory when herd movements would have influenced hunter-gatherer use of the steppes. This paper proposes four patterns of seasonal herd mobility for G. subgutturosa centred on Jordan's Azraq Basin. The four patterns are modelled using oxygen, carbon and strontium stable isotopes. Seasonal environmental signatures of each are understood through carbon and strontium isotopic variation in sixty modern plant specimens collected from twelve selected locations in north Jordan, published data on oxygen isotopes in local precipitation, and the adaptive behaviour of G. subgutturosa. The integrated isotopic datasets provide clear discriminatory markers for each proposed mobility pattern. Results will be applied in future to isotopic data from archaeological gazelle teeth from the Azraq Basin.
Additional Information:	
Question	Response
Author Comments:	Dear Dr Mighall, Confidential note re our submission in regards to peer reviewing

Title page

The seasonal mobility of prehistoric gazelle herds in the Azraq Basin, Jordan: modelling alternative strategies using stable isotopes

1. Introduction

Stable isotope data retrieved from wild ungulate archaeological teeth have been used to great effect to elicit their seasonal diet and mobility; studies allow informed inference on past hunting strategies, occupation seasonality and settlement patterns (Britton et al 2009; Fenner 2008; Julien et al 2012). Archaeo-isotope data have the potential to provide information on seasonal herd movement that cannot simply be projected on the past from observation of modern herd behaviour due to animal behavioural plasticity (Julien et al 2012); inferences about wildlife behaviour taken from the historical records are also highly problematic when used for predictions about the deep past, due to the effects of human impacts, landscape degradation and range fragmentation (Martin 2000).

Isotopic approaches rest on understanding how environmental influences produce isotopic signatures of seasonal landscapes (Hobson 1999; Hoppe et al 1999). The construction of baselines using modern data provides the most robust understanding of these environmental influences; there are two ways to proceed. One approach is suited to the identification of a wide range of human and animal activities associated with unknown and subtle regional and chronological differences in palaeoecological locations and climatic conditions. This approach aims to map, at high resolution, microscale variation in isotopic ratios throughout the whole study region in all seasons and in different modelled climate regimes (eg Hartman & Danin 2010; Hartman & Richards 2014). The second approach first defines the limits of its enquiry by identifying likely locations, seasonal variation, movement patterns or animal species adaptability before constructing a focused isotopic baseline (eg Balasse et al 2002; Bogaard et al 2014; Britton et al 2009, Elliot et al 2014; Hoppe et al 1999; Julien et al 2012). In this study we take the second approach, modelling isotopic changes expected across the seasons of an annual cycle, along identified broad topographic routes that we hypothesise may have been seasonally traversed by a single ungulate taxon, the gazelle, itself well-studied ethologically.

Our focus is on the steppe/deserts of East Jordan, specifically the Azraq Basin, where a sequence of well-researched sites from the early Epipalaeolithic to early Neolithic (28,000-9000 cal BP) demonstrate often extreme dependence on gazelle hunting (Betts 1993; Martin et al 2016; Garrard and Byrd 2013). Questions abound as to the nature of hunter-gatherer occupation of the steppe/desert areas in prehistory, such as whether the resource base allowed only seasonal use, or more year-round settlement (Garrard and Byrd 2013; Maher et al 2012), and how far back into prehistory gazelle intercept mass-capture techniques extend (Betts 1993). There are therefore compelling reasons for better understanding past gazelle seasonal mobility in the study location. While zooarchaeological data informs on the results of hunting encounters, it cannot inform on prey wider annual mobility.

The study presented here aims to identify and model isotopic variation in the seasonal environments of four alternative hypothesised gazelle mobility patterns in and around the Azraq Basin. There is no agreement on ancient gazelle herd behaviour and mobility in this area: models of long distance gazelle migration remain influential (Henry 1995; Legge & Rowley-Conwy 1987), while ecological predictions might see herds better adapted to remain year round in a comparatively un-degraded and better resourced landscape (Jones & Richter 2011; Martin 2000; Zohary 1966). In the absence of extant gazelle in the region, and with an adherence to behavioural ecological principles that species mobility is ecologically adaptive rather than fixed (Davies et al 2012), we develop four likely gazelle mobility scenarios, and model the isotopic signatures of gazelle mobility patterns. This is achieved through integration of new isotope data retrieved from modern plants in the Azraq Basin with published datasets. The study establishes a baseline of targeted environmental signatures in preparation for future application with archaeological gazelle dental isotopes.

2. Azraq Basin: background

2.1 The Palaeoenvironment (Fig.1)

The Azraq Basin centres on an Oasis (c.520masl), an area of saline Quaternary gravel plains with, until recently, spring-fed permanent marshlands, seasonally inundated with wadi run-off (Ames & Cordova 2015). To the west/ south-west, Early Tertiary limestone plains grade into hills incised by seasonal streams. Pliocene Basalt boulder fields, also incised by wadi systems, cover the north/ north-eastern sector, and further west, beyond the Azraq drainage basin, Cretaceous limestone Jordanian Highlands rise to c850masl (Bender 1974).

Since the Last Glacial Maximum (LGM), the dominant weather system in north Jordan has tracked eastwards, bringing rain on south/south-westerly winds in cold seasons and effectively none in highly evaporative hot seasons (Enzel et al 2008). Climate reconstructions suggest LGM effective moisture was greater although cooler than today, but decreased post-LGM (Hunt & Garrard 2013; Jones & Richter 2011). There is no Azraq Basin signature for the Bölling-Allerød and Younger Dryas, but south Levantine evidence indicates a sequence of moist warmer conditions, a cool, drier event, then more humid conditions in the early Holocene (Robinson et al. 2006).

Zohary (1966) argues for species richness in the LGM similar to today but, before over-grazing, more abundant woody thickets fringing waterbodies and annual grasses blanketing interfluvial areas in spring, but less abundant halophytic species in summer. In cooler, moister periods, LGM palaeovegetation zones have been modelled to show an eastward isohyet shift, with mesic woodlands at >400mm, xeric parklands >200mm, steppe >100mm and desert <100mm (Hillman 1996; Hunt & Garrard 2013). Regional zooarchaeological results support this ecological characterization (Martin et al 2016), Irano-Turanic vegetation communities are evident in archaeobotanic assemblages (Colledge 2001), and geoarchaeological evidence shows reduced wetland areas persisting in dryer periods (Jones & Richter 2011).

2.2 Human activity

Extensive archaeological research reveals continuous human presence in the Azraq Basin post-LGM. Smaller sites appear to have been occupied in single seasons by hunter-gatherers, whereas occupation in more than one season was possible at large Early/Middle Epipalaeolithic aggregation sites (Garrard & Byrd 2013). Abandoned by the Late Epipalaeolithic, smaller seasonal sites again emerged to continue into the Neolithic (Richter & Maher 2013).

Zooarchaeology in the Azraq Basin attests to gazelle-rich hunting grounds post-LGM (Martin et al 2016). Gazelle remains are identified where possible to the Persian gazelle (*Gazella subgutturosa)* (hereafter gazelle) by horn core morphology (Martin et al 2010), rather than to the other steppic species, the Sand gazelle (*G. marica*, prevalent in Arabia today, Wacher et al 2010). Body part data indicate hunting relatively local to sites, with cull-pattern data suggesting hunting pressure on gazelle herds only in early Neolithic (Martin et al 2016).

2.3 Gazelle seasonal mobility

The focus on gazelle hunting begs questions about their seasonal distribution. Ramsey and Rosen (2016) argue the Oasis provided water-fed resources to humans and prey moving through the area, and in drier periods provided a refuge from the surrounding steppe; certainly, gazelle thrived in the Azraq Basin until local 20thC extinction. How far herds moved seasonally remains unexplored; their year-round presence could underpin multi-seasonal site occupation and a permanent human presence, whereas a seasonal migration passage would have attracted hunter/gatherers only seasonally.

The debate on gazelle seasonal mobility in the prehistoric Levantine steppes has drawn on indirect indicators: zooarchaeology, ethological reasoning, and historical record analogy. The possibilities are developed into four models, each centring on the Azraq Basin. Each are the subject of isotopic modelling that follows.

3. Four models of gazelle mobility (*Fig. 2*)

3.1 Year round presence

G. subgutturosa is highly adapted to steppe-desert habitats (Baharav 1981; Heptner et al 1988, 618-622), meeting water needs from food, synchronising birthing to essential grasses florescent in springtime, and selecting plants for moisture in summer. In seasonal climates, animals aggregate in large herds in winter but disperse into small groups in late spring to regulate body temperature, provide security for young, and follow patchier food resources. Regular, small-scale movement (a few km/day) between resource patches is common in well-resourced areas.

3.11 Seasonal aggregation and dispersal local to Azraq Basin (Fig. 2, Pattern 1). In light of past greater resource availability, Martin (2000) draws on gazelle ethology to argue a year round gazelle habitat in the Azraq Basin, with a pattern of aggregation in late autumn/over winter nearer the central Oasis, and localised dispersal in late spring/summer. Following this model, gazelle populations would have been locally available to hunters year-round.

3.2 Seasonal presence

Gazelle mobility increases as an adaptive response to greater resource patchiness. Movement (15-20km/few days) follows resources but becomes more linear, usually towards water, often uphill (Heptner et al 1988, 623). More rapid movement, responding to snow cover or predator danger crosses resource patches becoming truly migratory (Julien et al 2012). Human presence can lead to habitat fragmentation, forcing herd migrations between seasonal resource areas (Ito et al 2013). The following three models have gazelle only seasonally present in the Azraq Basin.

3.21 Westwards summer movement into Jordanian Highlands (Fig. 2, Pattern 2). Many ungulates move uphill in summer where the plant growing season is longer, returning downhill for winter shelter. Henry (1995, p371) suggests, in the Southern Levant, resource factors influencing wildlife movement were identical to those for transhumant herders. Therefore we consider a movement pattern where gazelle winter near the Oasis, but in summer follow resources along westerly/north-westerly wadi systems to cooler Jordan Highlands. That said, two isotope studies from prehistoric sites in the Jordan Highlands show that Natufian gazelle (Shewan 2004) and PPNA domestic caprine (Makarewicz 2014) remain in their local ecological zone.

3.22 Northward migrations to the mid-Euphrates (Fig 2. Pattern 3). The dominant model of gazelle seasonal mobility is proposed by Legge and Rowley-Conwy (1987) for the Syrian Euphrates late Epipalaeolithic. As zooarchaeological analyses indicate highly seasonal, late spring mass kills near Abu Hureyra, they argue herds migrated 600kms north to the mid-Euphrates (c300masl) in late spring to give birth in better-watered habitats, then returned south in small groups to winter in the Azraq Basin. In support of migratory behaviour, the authors draw on ethno-historic accounts of gazelle racing past human settlements, and suggest this behaviour explains the locations of later widespread mass-capture ‘desert kite’ structures (Betts 1993).

Many archaeologists have adopted this gazelle migration model (Bar-Oz et al 2011; Goring-Morris 1995, 156), although Early Holocene Göbekli Tepe (Upper Euphrates) gazelle strontium isotope evidence shows little indication of herd movement extending as far south as the basalt shield - a barrier before the Azraq Basin (Lang et al 2013, 24). We base our model of seasonal migration on Legge and Rowley-Conwy’s (1987) description.

3.23 South-eastward movement along Wadi Sirhan (Fig. 2, Pattern 4). A second steppic species, *G.marica* is known from South Arabia, which is linked to the Azraq Oasis along the Sirhan depression. This 300km south-easterly corridor runs along the basalt edge and is fed by wadis and springs, with lake formation in wetter periods (Breeze et al 2016). It is of interest to scholars studying early human movement (Petraglia & Alsharekh 2003), gazelle too could have moved along the string of resource-rich areas (Stimpson et al 2016).

In this fourth scenario, in a reversal of seasonal movement described in the previous two, gazelle movement is modelled from cooler summer grounds around the Oasis, southeast along Wadi Sirhan, to warmer winter grounds around the Nefud Desert.

4. Isotopic variation in the North Jordan landscape

Oxygen, carbon and strontium isotopic ratios have the potential to discriminate between seasonal environments of the four proposed gazelle movement patterns due, respectively, to the region's climate seasonality (Dansgaard 1964; Rozanski et al 1993), the range of vegetation aridity-management strategies (Ehleringer et al 1997; O'Leary 1988; Vogel et al 1986), and the variety of distinct geological substrates (Faure & Powell 1972).

4.1 The modern landscape

4.11 Oxygen isotopic markers of season and elevation (*Fig. 3*). Global Natural Isotopes in Precipitation monthly records have partial $\delta^{18}O$ data, but the annual trajectory suggests enriched summer peaks in hot, arid seasons contrasting with winter troughs in cold, rainy seasons. Ranges extend from >0.57‰ to -6.32‰ in the Azraq Oasis, and >-3.32‰ to -7.28‰ for Ras Muneef in the Jordanian Highlands (IAEA/WMO 2014). Ras Muneef has more depleted ^{18}O throughout, as expected in a location of greater precipitation, lower temperatures and nearer oceanic precipitation sources. Outside the wet season, ^{18}O depletion exceeds the modelled ~0.28‰/100m rise in elevation (Poage & Chamberlain 2001).

4.12 Carbon isotopic markers of vegetation type. In the study area we can expect most grasses to have C_3 photosynthetic pathways and most C_4 species to be perennial chenopods. Short-lived spring annuals, constituting 80% of Azraq Basin species (Zohary 1974), have C_3 photosynthetic pathways (Bocherens et al 2001; Vogel et al 1986), as do slower growing shrubs and trees; these would return $\delta^{13}C$ ~-27‰ (O'Leary 1988). Halophytic chenopods, predominant throughout the arid season, have C_4 photosynthetic pathways with ^{13}C enriched to ~-12‰ (Akhani et al 1997; Shomer-Ilan et al 1981).

Whilst C_4 species do not exhibit water-stress induced $\delta^{13}C$ changes during arid seasons, C_3 taxa $\delta^{13}C$ might vary as much as 7.7‰ (Heaton 1999; Tieszen & Boutton 1989); raised water-stress, temperature, light levels, and elevation enrich ^{13}C, whereas tree canopy and water-body proximity deplete it. Opportunist annuals have depleted ^{13}C as they complete growth during the wet season, whereas dry-season growth in other species would have more enriched values (Hartman & Danin 2010).

4.13. Strontium isotopes markers of location. Only the labile fraction of bedrock strontium enters the food chain. Shewan (2004) identifies a gradient of variation in $^{87}Sr/^{86}Sr$ in modern plants and small herbivores consistent with variation in north Jordan geologies; high values (0.70798-0.70829) are associated with Cretaceous limestone and lower values (0.70702-0.70788) with basalt flows.

4.2 The Palaeolandscape

Regional post-LGM persistence of a seasonal climate is key to understanding isotopic signatures of past seasonal environments. As modern precipitation and vegetation patterns would have pertained, seasonal $\delta^{18}O$ and $\delta^{13}C$ can be expected. However, chronological variation in temperature and aridity would be expressed as isotopic value shifts; in $\delta^{18}O$ this would directly reflect changing temperature and aridity, whereas in $\delta^{13}C$, shifts would reflect changing C_3 species water-stress, and/or seasonal/zonal shifts in C_4/ C_3 species dominance.

Turning to strontium, soils in arid regimes largely derive from underlying bedrock (Bentley 2006), but where geologies intersect, upland sediments wash downstream or windborne dust settles (Graustein 1989; Sillen et al 1998), the resultant labile $^{87}Sr/^{86}Sr$ reflects the contributory mix. In the Azraq Basin this would be most marked in alluvial areas, where the basalt thins out over underlying Tertiary limestones, and where south/south-westerly prevailing winds transport dust onto downwind basalt fringes. Chronological climate aridity variation affects this mix, notably in windblown dust contribution. In arid periods dust is transported to the Azraq Basin from as far as North Africa (average $^{87}Sr/^{86}Sr$ 0.7085) (Gvirtzman & Wieder 2001; Stein et al 2007), however, its contributory effect on rendzina soil $^{87}Sr/^{86}Sr$ is minimal where precipitation is <150mm (Hartman & Richards 2014).

5. The modern baseline

In order to construct an isotopic model of the four gazelle movement patterns, further isotopic information from a small plant baseline adds detail to published data.

5.1 Methods

Our methods follow those of archaeological isotope scientists (Balasse et al 2002; Bogaard et al 2014; Elliot et al 2014; Hoppe et al 1999). Uncontaminated plants are readily available and no less useful than archaeological material (Balasse et al 2014) and in the Levant, provide accurate $^{87}Sr/^{86}Sr$ information on labile strontium distribution (Hartman & Richards 2014).

5.11 Collection protocols. Plants were collected for two studies, each determining collection and analytical protocols (*Fig 4, Supp. 1*). To define a seasonal $\delta^{13}C$ signature for gazelle forage, we collected in the main vegetation, hydrological and topographical settings. Multiple specimens of all grass and chenopod taxa were collected through field-walking. Their $\delta^{13}C$ was measured to establish signatures fine-tuned to the study region. In order to investigate how labile $^{87}Sr/^{86}Sr$ might provide locational signatures, a plant collection was made near key Epipalaeolithic and Neolithic sites that were located both deep within main regional geologies and where strontium sources were predicted to be most mixed. All locations avoided modern contaminants derived from traffic, herding, human occupation, industrial activity and water pollution.

The collection period was restricted to April 2013 and only the current season's growth was gathered, controlling for inter-annual atmospheric CO_2 variation. It was unnecessary to collect in other seasons as all C_3 grass growth occurs in the wet season and as C_4 species have unchanging $\delta^{13}C$ seasonally. Specimens were all moderately shallow-rooted, controlling for soil depth $^{87}Sr/^{86}Sr$ variation. Three individual specimens of the same species contributed to each sample.

Each plant was photographed (*Supp. 2*), and a record made of dimensions, maturity, habit, vegetation community, bedrock, soil quality, location aspect, current weather and soil conditions, UTM location and elevation (*Supp. 3*). Plants were identified using the British Institute for Archaeology in Amman reference collection and library, then exported with the permission of the Department of Antiquities of Jordan to UCL Institute of Archaeology for isotopic analyses.

5.12 Analytical protocols. Specimens were washed in Milli-Q water and aiar-dried in paper bags. Specimens for carbon isotope analyses were finely chopped, homogenised and freeze-dried before analysis at UCL Bloomsbury Environmental Isotopes Facilities in a Flash EA 1112 by gas chromatographic separation linked to a continuous flow IR-mass spectrometer (Thermo Delta V). Analytical error = 0.1‰. Strontium isotope preparation and analyses were conducted in a clean laboratory at the Earth Sciences Department, Royal Holloway College UL, by VG354 thermal ionisation mass spectrometer. Typical $^{87}Sr/^{86}Sr$ external reproducibility = ±0.000014 (2sd).

5.2 Results and interpretation (*Supp. 4*)

5.21 Grass and chenopod collection. Field walking retrieved eight chenopods, eight grasses and two wetland monocots. All grasses save one have C_3 photosynthetic pathways, and all chenopods are C_4

halophytes (*Supp 4, last column*). This species array is consistent with Irano-Turanic plant communities adapted to cold, wet winters and hot, arid summers.

5.22 *Carbon isotope results* (*Fig. 5*). The grasses and chenopods fall into two $\delta^{13}C$ groups ($P<0.00001$). The group to the left (N=10), has $\delta^{13}C$ -30.8‰ – -24.8‰ (mean -28.06±3.4 (2sd)) and the group to the right (N=9) has enriched ^{13}C -14.8‰ – -11.4‰ (mean -13.4±2.52 (2sd)). The $\delta^{13}C$ of each group is consistent with C_3 and C_4- species, which divide as predicted into monocots and chenopods (with the exception of *Cynodon dactylon*). Analyses allow $\delta^{13}C$ parameters relevant to regional gazelle feeding to be modelled. After an adjustment of -1.2‰ is made for modern atmospheric carbon dioxide (Friedli et al 1986), (LGM and Early Holocene atmospheric CO2 concentrations are thought to have been broadly similar (Tornero et al 2016)), the means of the two groups are used to establish the $\delta^{13}C$ of C_3 monocots at 26.86±3.4 (2sd) and C_4 chenopods at -12.2±2.52 (2sd).

5.23 Strontium isotope results (*Fig. 6*). Analyses of 41 plant samples from 12 locations produced an $^{87}Sr/^{86}Sr$ 0.70854–0.70764, which falls within published Jordanian limestone and basalt-rich ranges. Intra-sample variation tested in duplicate analyses (N=6) was found to be negligible (2 x 0‰, 3 x 0.00001, 1 x 0.00002).

Twenty-one $^{87}Sr/^{86}Sr$ results for four locations deep within major geologies range as follows; Cretaceous limestone (*location 1*, N=3) 0.70845–0.70854 (mean 0.70849±0.00009 (2sd)), Tertiary limestone (*location 3*, N=6) 0.70807–0.70819 (mean 0.70815±0.00011 (2sd)), Quaternary gravels (*locations 4 & 5*, N=6) 0.70807–0.70816 (mean 0.70811±0.00007 92sd)) and basalts (*location 11*, N=6) 0.70764–0.70778 (mean 0.70772±0.00012 (2sd)). Cretaceous and Tertiary limestone means differ by 0.00034, Quaternary gravels and basalt means by 0.00039, but Tertiary limestones and Quaternary gravels only by 0.00004. In order to define strontium isotopic signatures for the four gazelle mobility patterns, we establish Jordanian Highlands and basalt endmember signatures using the above values. However, we amalgamate Tertiary limestone and Quaternary gravel $^{87}Sr/^{86}Sr$ signatures (N = 12, mean 0.70813±0.00009 (2sd)) to model together the limestone steppe and its overlying fluvial deposits. Significant variation (Anova) between these three groups $P<0.00001$.

In order to investigate $^{87}Sr/^{86}Sr$ signatures in locations with the greatest predicted contributory mix, a further twenty results were retrieved from seven other locations. Results (*Fig. 7*) are ordered to follow a broad south-west/north-east locational trajectory. The $^{87}Sr/^{86}Sr$ results along this trajectory are progressively depleted, consistent with predicted changes in contributory endmember mixing and/or windblown dusts.

Wadi Zarqa Ma'in (*Fig.4, location 2*) mean $^{87}Sr/^{86}Sr$ is 0.7082, between Tertiary and Cretaceous limestone signatures, which reflects its Highlands-edge location. Wadi Ruwayshid (*location 12*) mean $^{87}Sr/^{86}Sr$ is 0.7083, a limestone signature reflecting its position on the highly deflated eastern limestone steppe. On the basalt, Wadi el Ghusein (*location 9*) and Burqu (*location 10*) have $^{87}Sr/^{86}Sr$ means, respectively 0.70783 and 0.70787, which are higher than the deep basalt endmember signature, but lower than Dhuweila (*location 7*) and the Tapline Road south of Safawi (*location 6*) means, respectively, 0.70806 and 0.70795, further west near the basalt edge.

Variation between the $^{87}Sr/^{86}Sr$ signatures of these intermediary points is not significant although, for the purposes of modelling gazelle mobility patterns, they serve as a reminder that individual locations cannot be precisely identified, but do support expected trajectories in $^{87}Sr/^{86}Sr$ accompanying progression from one geology to another.

6. Discussion

6.1 Isotopic modelling of four gazelle mobility patterns

Isotopic signatures can now be applied to the four mobility patterns (*Section 3*). Each has its own set of seasonal $\delta^{18}O$, $\delta^{13}C$ and $^{87}Sr/^{86}Sr$ (*Table 1, Fig. 8*). Signatures associated with the first model of minimal herd movement throughout the year are, to aid discussion, taken as the starting point.

The shape of each isotopic curve is of key interest, illuminating progressive changes throughout seasons and across geologies. Azraq and Ras Muneef $\delta^{18}O$ in precipitation (*Section 4.11*) provides guidelines to likely locational seasonal values and elevation effects. The $\delta^{13}C$ of regional C_3 grasses and C_4 chenopods (*Section 5.22*) provide endmembers to modelled curves of seasonally available vegetation suited to gazelle ethology. Labile $^{87}Sr/^{86}Sr$, measured in our plant baseline (*Section 5.23*) provides endmembers to modelled geological location, alongside guidelines to progressive mixing in the Azraq Basin.

6.11. Seasonal aggregation and dispersal local to Azraq Oasis (Pattern 1)

The modelled annual $\delta^{18}O$ curve is clearly sinusoidal, with depleted winter troughs and enriched summer peaks, reflecting regional climate seasonality. There is no seasonal signature loss associated with areas of different temperature and aridity. The $\delta^{13}C$ annual sequence is also sinusoidal as opportunist C_3 grasses, dominant after winter rains, flourish before giving way in summer to water-stressed C3 shrubs and arid-adapted C_4 halophytes. As this pattern sees minimal movement, $^{87}Sr/^{86}Sr$ remains unchanged throughout the year, with values in the Tertiary Limestone/Quaternary Gravels band.

	Autumn	Winter		Spring		Summer		Autumn
	late	early	late	early	late	early	late	early
Local aggregation/ dispersal around Oasis (1)	**large herd aggregation -Oasis protection**				**birthing/ small group dispersal into steppe**			
Seasonal climate – temperature, water availability	$\delta^{18}O$ falling - dew/ temp	trough $\delta^{18}O$ - cold, wet season		rising with temp, rains ease		peak $\delta^{18}O$ - highest temp/ aridity		$\delta^{18}O$ falling - dew/ temp
Seasonal food – preference/ availability	peak enriched ^{13}C - C4 chenopods		falling $\delta^{13}C$ –C3 flush	trough lowest $\delta^{13}C$ - C3 grasses dominate		rise $\delta^{13}C$ - C3s wither	peak $\delta^{13}C$ -C4 chenopods retain moisture	
Seasonal location – geological soil inputs	$^{87}Sr/^{86}Sr$ Tertiary Limestone /Quaternary gravel all year							
Westwards movement to Jordanian Highlands (2)	**down wadis to Oasis**	**large herd aggregation - Oasis protection**			**birthing/ up W/NW wadis**		**dispersed groups, cooler Jordanian Highlands**	
Seasonal climate – temperature, water availability	As in pattern (1)					summer peak lost - altitude temps cooler/ better watered		
Seasonal food – preference/ availability	As in pattern (1)					summer peak lost - longer C3 growing season, less water stress, less C4		
Seasonal location – geological soil inputs	$^{87}Sr/^{86}Sr$ falls nearer Tertiary Limestone	$^{87}Sr/^{86}Sr$ trough – maximum Tertiary Limestone /Quaternary gravel				$^{87}Sr/^{86}Sr$ rises nearer Cretaceous Limestone	$^{87}Sr/^{86}Sr$ peak -maximum Cretaceous Limestone contribution	
Northward migration to Mid-Euphrates (3)	**group south migration**	**overwinter near protected Oasis**		**herd north migration**	**birthing / feeding in lusher Mid-Euphrates**			**group south migration**
Seasonal climate – temperature, water availability	As in pattern (1)					summer peak lost - north temps cooler, better watered		
Seasonal food – preference/ availability	As in pattern (1)					summer peak lost – longer C3 growing season, less water stress, C4 predominate less		
Seasonal location – geological soil inputs	$^{87}Sr/^{86}Sr$ lowest - returning across basalt	$^{87}Sr/^{86}Sr$ - Tertiary Limestone/ Quaternary gravel		$^{87}Sr/^{86}Sr$ lowest - heading north across basalt		$^{87}Sr/^{86}Sr$ - northern Tertiary Limestone/ Quaternary gravel		87Sr/86Sr lowest returning across basalt
South-eastwards movement along Wadi Sirhan (4)	**move south along W. Sirhan**	**over-wintering - warm Nefud desert**		**move north along W. Sirhan**	**birthing/ feeding - cooler, better watered Oasis**			**move south along W. Sirhan**
Seasonal climate – temperature, water availability	Depleted ^{18}O - winter troughs lost, arid desert			As in pattern (1)				
Seasonal food – preference/ availability	Enriched ^{13}C - arid desert, C4 plants outcompete C3			As in pattern (1)				
Seasonal location – geological soil inputs	$^{87}Sr/^{86}Sr$ Tertiary Limestone / basalt mix	$^{87}Sr/^{86}Sr$ Nefud Tertiary Limestone /Quaternary		$^{87}Sr/^{86}Sr$ Tertiary Limestone / basalt mix	87Sr/86Sr Oasis Tertiary Limestone /Quaternary gravel			$^{87}Sr/^{86}Sr$ Tertiary Limestone / basalt mix

Table 1. Seasonal changes in $\delta^{18}O$, $\delta^{13}C$ and $^{87}Sr/^{86}Sr$ modelled for proposed gazelle mobility patterns in Figure 2

6.12. Westwards summer movement into Jordanian Highlands (Pattern 2)

In this pattern, gazelle herds overwinter around the Azraq Oasis, therefore winter isotopic signatures are similarly modelled. As summer is spent at higher elevations, enriched ^{18}O and ^{13}C associated with hot, arid conditions around the Oasis are largely lost and a reduced summer seasonal signature is modelled. The $^{87}Sr/^{86}Sr$ annual sequence is sinusoidal, with values rising in late spring as herds approach Cretaceous Limestone uplands, then falling with late autumn downhill return.

6.13. Northward migration to the mid-Euphrates (Pattern 3)

In this pattern, as previously, gazelle herds overwinter in the Azraq Basin. The $\delta^{18}O$ and $\delta^{13}C$ for late spring and summer further north at higher elevations in the mid-Euphrates, are also lower. However, the $^{87}Sr/^{86}Sr$ curve has a very different undulating profile, with values now falling towards those for basalt, once in spring and again in autumn as herds cross to and from the mid-Euphrates.

6.14. South-eastward movement along Wadi Sirhan (Pattern 4)

Here, summer isotopic signatures are now those of the Azraq Basin, as herds move to this better-watered location avoiding extreme heat and aridity further south. Winter is spent in the warmer, drier Nefud where vegetation is more arid-adapted; modelled ^{18}O and ^{13}C remain enriched, losing much of the depleted seasonal Azraq signature. Away from the Azraq Basin, modelled $^{87}Sr/^{86}Sr$ might show a slight depletion as Wadi Sirhan follows the southern basalt edge. However, given expected Tertiary limestone dust contribution from the south/southwest, significant seasonal variation is not predicted.

6.2 Application of the model

The combined package of seasonal isotopes for each mobility pattern is unique, able to offer stand-alone signatures distinguishing each. The strength of studying all three datasets in combination lies in the interplay of environmental information that reduces each dataset's interpretive problems; location may be approached through both $\delta^{18}O$ and $^{87}Sr/^{86}Sr$, seasonality through both $\delta^{18}O$ and $\delta^{13}C$. For example, location, vegetation availability, temperature, humidity or tree cover might underlie $\delta^{13}C$ variation, but $^{87}Sr/^{86}Sr$ constrain location and $\delta^{18}O$ identifies seasonal stress factors.

Gazelle ethology further constrains interpretation. For example, other seasonal mobility patterns are unlikely in this region, where birthing requirements restrict seasonal behaviour and where summer feeding and thermo-regulation largely inform mobility. The most depleted ^{13}C signatures can be associated with feeding on spring grasses around birthing, and unchanging $^{87}Sr/^{86}Sr$ signatures suggest localised movement rather than longer journeys over the same geology serving no purpose, wasting energy and compromising thermo-regulation.

This research provides isotopic signatures of four likely seasonal mobility patterns of gazelle herds hunted by prehistoric occupants of the Azraq Basin. In future, these signatures will be compared to those in the teeth of archaeological gazelle found on occupation sites. As zooarchaeological analysis determines hunting was local to occupation sites, further constraints can be placed on $^{87}Sr/^{86}Sr$ location signature.

It is not the place of this paper to discuss gazelle dental isotope systematics, however certain aspects will allow strengthened interpretation of our seasonal mobility models in future archaeological application. Firstly, sequential sampling of gazelle teeth will provide an approximate one-year time capsule of isotope results, with individual data-point resolution greater than seasonal. Consequently, at this timescale, intra-tooth isotopic variation will relate to seasonal behaviour which can be associated directly with our annual mobility models. Long-term variation (climate induced dust amount ($^{87}Sr/^{86}Sr$), aridity and soil cover ($\delta^{13}C$), temperature and precipitation ($\delta^{18}O$)) would not register and can be discounted.

Secondly, $\delta^{18}O$ and $\delta^{13}C$ will be retrieved from the same enamel carbonate fraction, so a clear seasonal interpretation of the $\delta^{13}C$ will be provided by the temporally linked $\delta^{18}O$. Thirdly, archaeological samples will be retrieved from spatially and chronologically identified occupation sites, such that robust sample sizes will allow identification of difference associated with location, long-term climate variation, or human behaviour. Interpretation of $\delta^{18}O$ in particular is strengthened, as seasonality information, at present modelled on curve shape, might then allow some comparative quantification.

Conclusion

Four patterns of gazelle seasonal mobility in the prehistory of the east Jordanian steppe have been proposed. For each pattern, the seasonal and spatial progression has been identified in modern stable isotopes indicators taken from environmental data. In combination, the data provide distinguishing features for each pattern with clear trajectories associated with any changes in location and with seasonal changes in climate and food availability. The baseline study of strontium isotopes in modern plants is in agreement with predicted mixing effects and provides a modelled trajectory of changing values. This allows each long distance route away from the central Oasis to be identified and to be distinguished from the localised aggregation/ dispersal pattern.

Collection of isotopic data is already underway from 112 gazelle teeth retrieved from 12 archaeological sites which encompass a range of spatial and chronological prehistoric occupations in the Azraq Basin. The baseline described in this paper is intended for use in future research, where it will be an invaluable resource for the interpretation of the archaeological data, such that the seasonal movement of prehistoric gazelle herds, and their availability to hunters can be discussed.

Acknowledgements

We are grateful to Department of Antiquities, Jordan, for allowing specimen collection and export, and Osama Lutfi, Jordanian Government Representative, for fieldwork assistance.

References

Akhani, H., Trimborn, P. Ziegler, H. 1997. Photosynthetic pathways in *Chenopodiaceae* from Africa, Asia and Europe *Plant systematics and evolution 206*, 187-221.

Ames, C., Cordova, C. 2015. Middle and Late Pleistocene landscape evolution at the Druze Marsh site in northeast Jordan. *Geoarchaeology 30*, 307-329.

Baharav, D. 1981. Food habits of the mountain gazelle in semi-arid habitats of eastern Lower Galilee, Israel. *J. Arid Environments 4*, 63-69.

Balasse, M., Ambrose, S., et al. 2002. The seasonal mobility model for prehistoric herders in the south-west Cape of South Africa assessed by isotopic analysis of sheep tooth enamel. *J. Archaeological Sciences 29*, 917-932.

Balasse, M., al Zaidaneen, J., et al. 2014. Tracing herding patterns at Ayn Abū Nukhayla through biogeochemical analyses ($\delta^{13}C$, $\delta^{18}O$, $^{87}Sr/^{86}Sr$) in faunal remains. In (Eds.) Henry, D., Beaver, J. *The sands of time*. *Ex oriente:* Berlin, 91-104.

Bar-Oz, G., Zeder, M., Hole, F. 2011. Role of mass-kill hunting strategies in the extirpation of Persian gazelle (*Gazella subgutturosa*) in the northern Levant, *PNAS 108*, 7345–7350.

Bender, F. 1974. *Geology of Jordan*. Berlin: Borntraeger.

Bentley, A. 2006. Strontium isotopes from the earth to the archaeological skeleton. *J Archaeological Method and Theory 13*, 135-187.

Betts, A. 1993. The Neolithic sequence in the east Jordan badia. *Paléorient 19*, 43-53.

Bocherens, H., Mashkour, M., et al. 2001. A new approach for studying prehistoric herd management in arid areas. *Earth and Planetary Sciences322*, 67-74.

Bogaard, A., Henton, E., et al. 2014. Locating land use at Neolithic Çatalhöyük, Turkey. *Archaeometry 56*, 860-877.

Breeze, P., Groucutt, H., et al. 2016. Palaeohydrological corridors for hominin dispersals in the Middle East ~250-70,000 years ago. *Quaternary Science Review 144,* 155-185.

Britton, K., Grimes, V., et al. 2009. Reconstructing faunal migrations using intra-tooth sampling and strontium and oxygen isotope analyses. *J. Archaeological Science 36*, 1163-1172.

Colledge, S. 2001. *Plant exploitation on Epipalaeolithic and early Neolithic sites in the Levant*. Oxford, BAR S986.

Dansgaard, W. 1964. Stable isotopes in precipitation. *Tellus 16*, 436-468.

Davies, N., Krebs, J., West, S. 2012. *An Introduction to Behavioural Ecology,* 4th Edition. Wiley-Blackwell.

Edwards, Y., Martin, L. 2007. Fauna from the Natufian and PPNA cave site of Iraq ed-Dubb. *Paléorient 33,* 143-174.

Elliott, S., Bendrey, R., et al. 2014. Preliminary ethnoarchaeological research on modern animal husbandry in Bestansur. *EA.* DOI 10.1179/1749631414Y.0000000025.

Enzel, Y., Amit, R., et al. 2008. The climatic and physiographic controls of the eastern Mediterranean over the late Pleistocene climates in the southern Levant and its neighbouring deserts. *Global and Planetary Change 60,* 165-192.

Faure, G., Powell, J. 1972. *Strontium Isotope Geology*. New York: Springer.

Fenner, J. 2008. The use of stable isotope ratio analysis to distinguish multiple prey kill events from mass kill events. *J. Archaeological Science 35*, 704-716.

Friedli, H., Loetscher, H., et al. 1986. Ice core record of the C-13/C12 ratio of atmospheric CO2 in the past two centuries. *Nature 324*, 237-238.

Garrard, A., Byrd, B. 2013. *Beyond the Fertile Crescent, Volume 1*. Oxford: Oxbow.

Garrard, A., Colledge, S., Martin, L. 1996. The emergence of crop cultivation and caprine herding in the ‘marginal zone’ of the southern Levant. In (Ed.) Harris, D. *The origins and spread of agriculture* *and pastoralism in Eurasia.* USA: Smithsonian Institute Press, 204-226.

Goring-Morris, N. 1995. Complex hunter-gatherers at the end of the Palaeolithic (20,000-10,000 BP), 142-167, in (Ed.) Levy, T. *The Archaeology of society in the Holy Land*, Leicester University Press.

Graustein, W. 1989. $^{87}Sr/^{86}Sr$ ratios measure the sources and flow of strontium in terrestrial ecosystems. In (Eds.). Rundel, P., Ehleringer, J., Nagy, K. *Stable Isotopes in Ecological Research.* Springer-Verlag, New York, 491–512.

Gvirtzman, G., Wieder, M. 2001. Climate of the last 53,000 years in the Eastern Mediterranean, based on soil-sequence stratigraphy in the coastal plain of Israel. *Quaternary Science Review 20*, 1827–1849.

Hartman, G., Danin, A. 2010. Isotopic values of plants in relation to water availability in the Eastern Mediterranean region. *Oecologia 162*, 837–852.

Hartman, G., Richards, M. 2014. Mapping and defining sources of variability in bioavailable strontium isotope ratios in the Eastern Mediterranean. *Geochimica et Cosmochimica Acta 126*, 250-264.

Heaton, T. 1999. Spatial, species, and temporal variations in the 13C/12C ratios of C_3 Plants. *J. Archaeological Science 26*, 637-649.

Heptner, V., Nasimovich, A., Bannikov, A. 1988. *Mammals of the Soviet Union, volume 1*. Washington: Smithsonian Institute.

Henry, D. 1995. *Prehistoric cultural ecology and evolution: insights from southern Jordan*. New York: Plenum Press.

Hillman, G. 1996. Late Pleistocene changes in wild plant-foods available to hunter–gatherers of the northern Fertile Crescent. In (Ed.) Harris D. *The origins and spread of agriculture and pastoralism in Eurasia.* Washington D.C.: Smithsonian Institution Press, 159-203.

Hobson, K. 1999. Tracing origins and migration of wildlife using stable isotopes: a review. *Oecologia 120*, 314-326.

Hoppe, K., Koch, P., et al. 1999. Tracking mammoths and mastodons. *Geology 27*, 439-142.

Hunt, C., Garrard, A., 2013. The Late Palaeolithic – geological context. In (Eds.) Garrard, A., Byrd, B., 2013. *Beyond the Fertile Crescent,Volume 1*. Oxbow Books, Oxford, pp. 53-135.

IAEA/WMO. 2014. Global network of isotopes in precipitation. *The GNIP Database.* http://www.iaea.org/water

Ito, T., Lhagvasuren, B., et al. 2013. Fragmentation of the habitat of wild ungulates by anthropogenic barriers in Mongolia. PlosOne 8:ee6995.

Jones, M., Richter, T. 2011. Paleoclimatic and archeological implications of Pleistocene and Holocene environments in Azraq, Jordan. *Quaternary Research* 76, 363-372.

Julien, M.-A., Bocherens, H., et al. 2012. Were European steppe bison migratory? *Quaternary International 271*, 106–119.

Lang, C., Peters, J., et al. 2013. Gazelle behaviour and human presence at early Neolithic Göbekli Tepe, south-east Anatolia. *World Archaeology 45*, 410-429.

Legge, A., Rowley-Conwy, P. 1987. Gazelle killing in Stone-age Syria. *SA 255*, 88-95.

Makarewicz, C. 2014. Bridgehead to the Badia. In (Eds.) Finlayson, B., Makarewicz, C. *Settlement, survey and stone*. Berlin: Ex Oriente, 117-131.

Maher, L.A., Richter, T., et al. 2012. Twenty thousand-year-old huts at a hunter-gatherer settlement in eastern Jordan. *PLoS One 7 (2), e31447*. http://dx.doi.org/10.1371/journal.pone.0031447.

Martin, L. 2000. Gazelle (*Gazella* spp.) behavioural ecology. *J. Zoology, London 250*, 13-30.

Martin, L., Edwards, Y.H., Garrard, A., 2010. Hunting practises at an eastern Jordan Epipaleolithic aggregation site: the case of Kharaneh IV. *Levant* 42, 107-135.

Martin, L., Edwards, Y., et al. 2016. Faunal turnover in the Azraq Basin, eastern Jordan 28,000 to 9,000 cal B. *Quaternary Research*, http://dx.doi.org/10.1016/j.yqres.2016.07.001.

O'Leary, M. 1988. Carbon isotopes in photosynthesis. *Bioscience 38*, 328–336.

Petraglia, M., Alsharekh, A. 2003. The Middle Palaeolithic of Arabia. *Antiquity 77,* 671-684.

Poage, M., Chamberlain, C. 2001. Empirical relationships between elevation and the stable isotope composition of precipitation and surface waters. *American Journal Science 301,* 1-15.

Ramsey, M., Rosen, A. 2016. Wedded to wetlands. *Quaternary International 396,* 5-19.

Richter, T., Maher, L. 2013. The Natufian of the Azraq Basin. In (Eds) Bar-Yosef, O., Valla, F. *Natufian foragers in the Levant.* Institute Monographs in Prehistory: Ann Arbor, 429-448.

Robinson, S., Black, S., et al. A review of palaeoclimates and palaeoenvironments in the Levant and Eastern Mediterranean from 25,000 to 5000 years BP. *Quaternary Science Reviews 25*, 1517-1541.

Rozanski, K., Araguas-Araguas, L., Gonfiantini, R. 1993. Isotopic patterns in modern global precipitation. *American Geophysics Union, Geophysics Monograph 78*, 1-36.

Shewan, L. 2004. Natufian settlement systems and adaptive strategies. In (Ed). Delage, C. *The last hunter-gatherer societies in the Near East.* BAR (International Series) 1320: Oxford.

Shomer-Ilan, A., Nissenbaum, A., Waisal, Y. 1981. Photosynthetic pathways and the ecological distribution of the *Chenopodiaceae* in Israel. *Oecologia 48*, 244-248.

Sillen, A., Hall, G., et al. 1998. 87Sr/86Sr ratios in modern and fossil food-webs of the Sterkfontein Valley. *Geochimica et Cosmochimica Acta 62*, 2463-2473.

Stein, M., Almogi-Labin, A., et al. 2007. Late Quaternary changes in dust inputs to the Red Sea and Gulf of Aden from $^{87}Sr/^{86}Sr$ ratios in deep-sea cores. *Earth Planetary Science Letters 261,* 104-119.

Stimpson, C., Lister, et al. 2016. Middle Pleistocene vertebrate fossils from the Nefud Desert, Saudi Arabia. *Quaternary Science Reviews 143*, 13-36.

Tieszen, L., Boutton, T. 1989. Stable carbon isotopes in terrestrial ecosystem research. In (Eds), Rundel, P., Ehleringer, J., Nagy, K. *Stable Isotopes in Ecological Research*. Springer-Verlag, New York, 167-195.

Tornero, C., Balasse, M., et al. 2016. The altitudinal mobility of wild sheep at the Epigravettian site of Kalavan 1 (Lesser Caucasus, Armenia). *J. Human Evolution 97,* 27-36.

Vogel, J., Fuls, A., Danin, A. 1986. Geographical and environmental distribution of C_3 and C_4 grasses in the Sinai, Negev, and Judean deserts. *Oecologia 70,* 258-265.

Wacher, T., Wronski, T., et al. 2010. Phylogenetic analysis of mitochondrial DNA sequences reveals polyphyly in the goitred gazelle (*Gazella subgutturosa*). *Conservation Genetics* 12, 827–831.

Zohary, M., Feinbrun-Dothan, N. 1966. *Flora Palestina.* Jerusalem: Israel Academy of Sciences and Humanities.

List of figures

Figure 1. Azraq Basin (black line) within Jordan (dotted line), showing geology, isohyets and cited site locations (a. Kharaneh, b. Ain Ghazal, c. Azraq Oasis, d. Shubayqa, e. Dhuweila, f. Wadi Jilat)

Figure 2. Modelled routes of four gazelle mobility patterns

Figure 3. GNIP Monthly records (A. Azraq, B. Ras Muneef precipitation and temperatures, C. Both, oxygen isotopes in precipitation)

Figure 4. Modern plant collection points (numbered) overlying geological features of Jordan (Supp. 1 for details)

Figure 5. Carbon stable isotope results for modern plant specimens, with published average $\delta^{13}C$ for C_3 and C4 species

Figure 6. Strontium isotope results for endmembers in and around the Azraq Basin

Figure 7. Strontium isotope results for locations with predicted mixed source contributions

Figure 8. Predicted changes in seasonal environments of proposed gazelle mobility patterns (Fig. 2) modelled using oxygen, carbon and strontium isotopic data, as outlined in:
Section 5.22 for $\delta^{13}C$:C_3 monocots 26.86±3.4 (2sd), C_4 chenopods -12.2±2.52 (2sd)
Section 5.23 for $^{87}Sr/^{86}Sr$: Cretaceous limestone 0.70849±0.00009 (2sd), Tertiary limestone and Quaternary gravel 0.70813±0.00009 (2sd), basalts 0.70772±0.00012 (2sd).
Seasonal oxygen curves are not assigned values, their shape being used to define seasons or loss of seasonality

Fig 1. ENVIRONMENT MAP

Click here to download Non-colour figure FIG. 1 ENVIRON MAP.tif

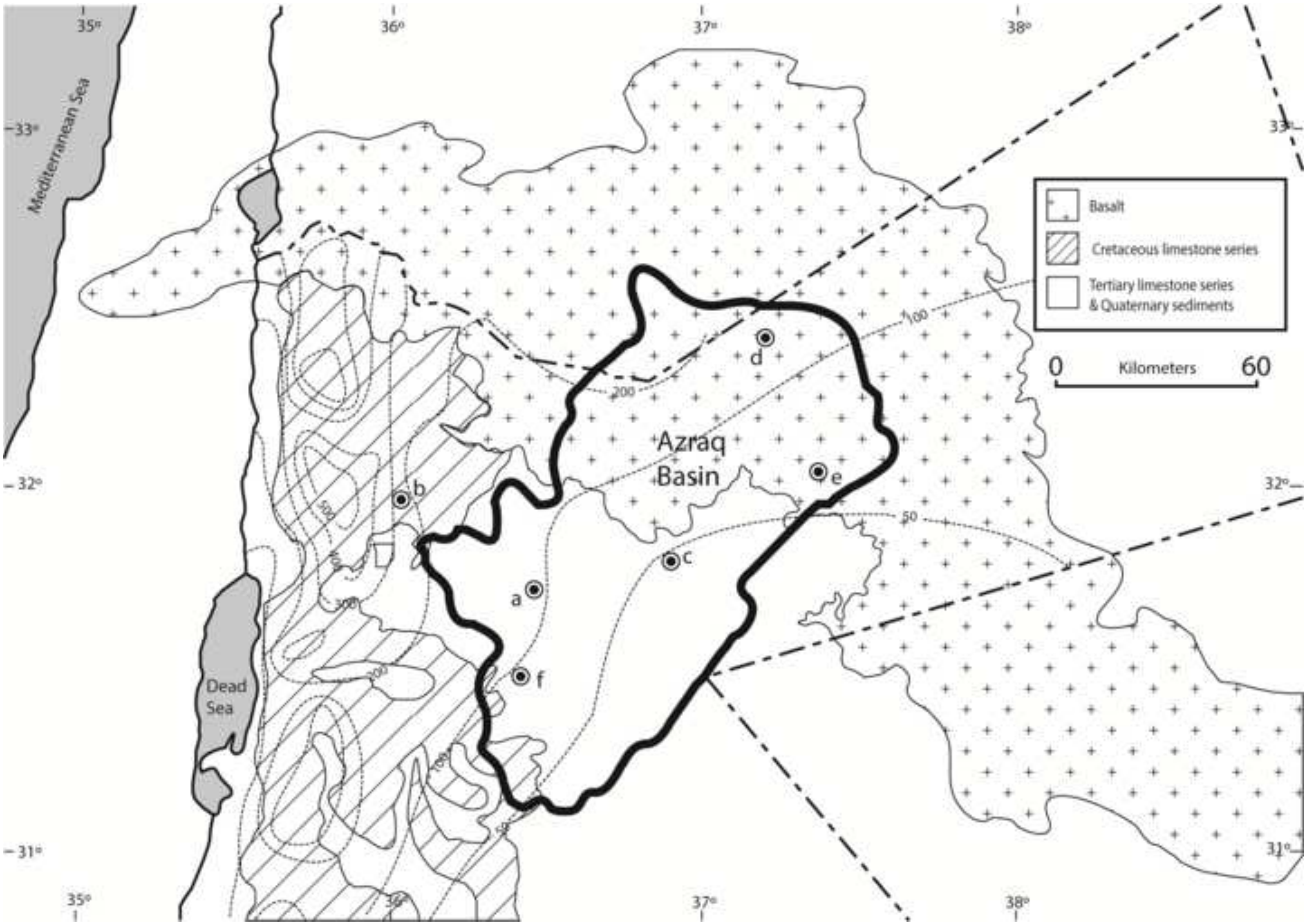

Fig 2. MOBILITY PATTERNS MAP

Click here to download Non-colour figure FIG. 2 MOBILITY PATTERNS MAP.tif

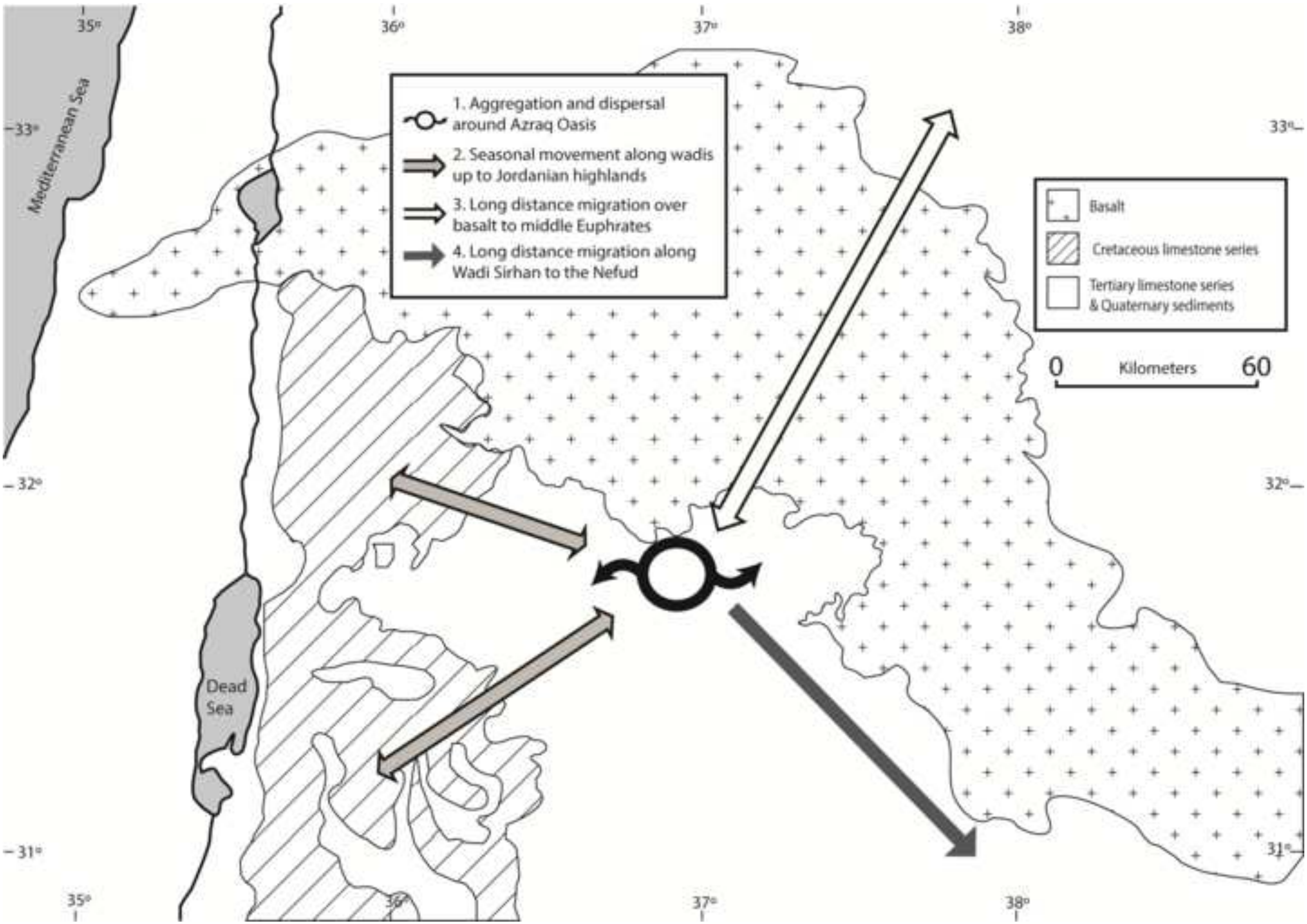

Fig 3 GNIP oxygen

Click here to download Non-colour figure Fig 3. GNIP oxygen charts.xlsx

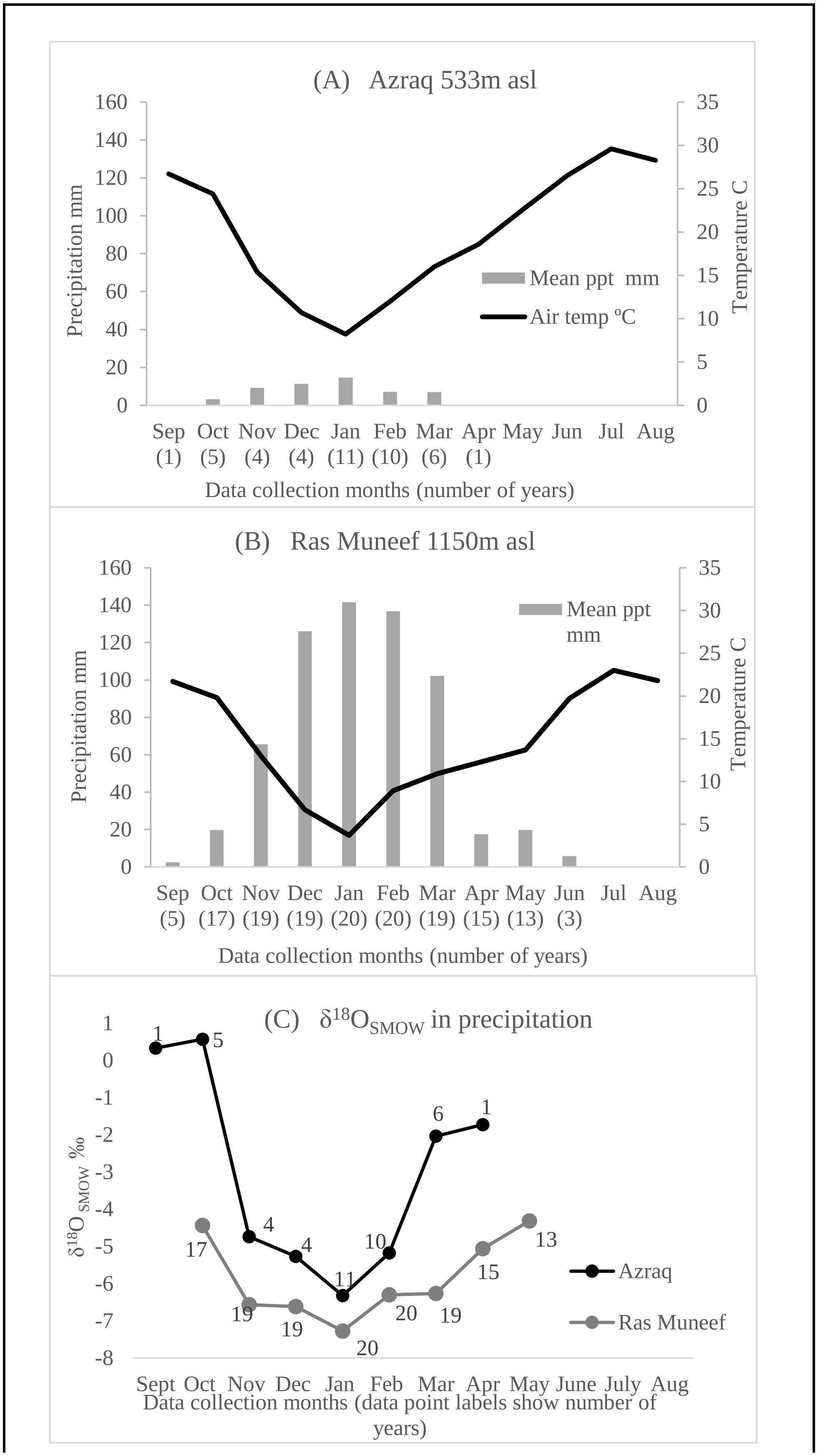

Fig 4. PLANT COLLECTION MAP

Click here to download Non-colour figure FIG. 4 PLANT COLLECTION MAP.tif

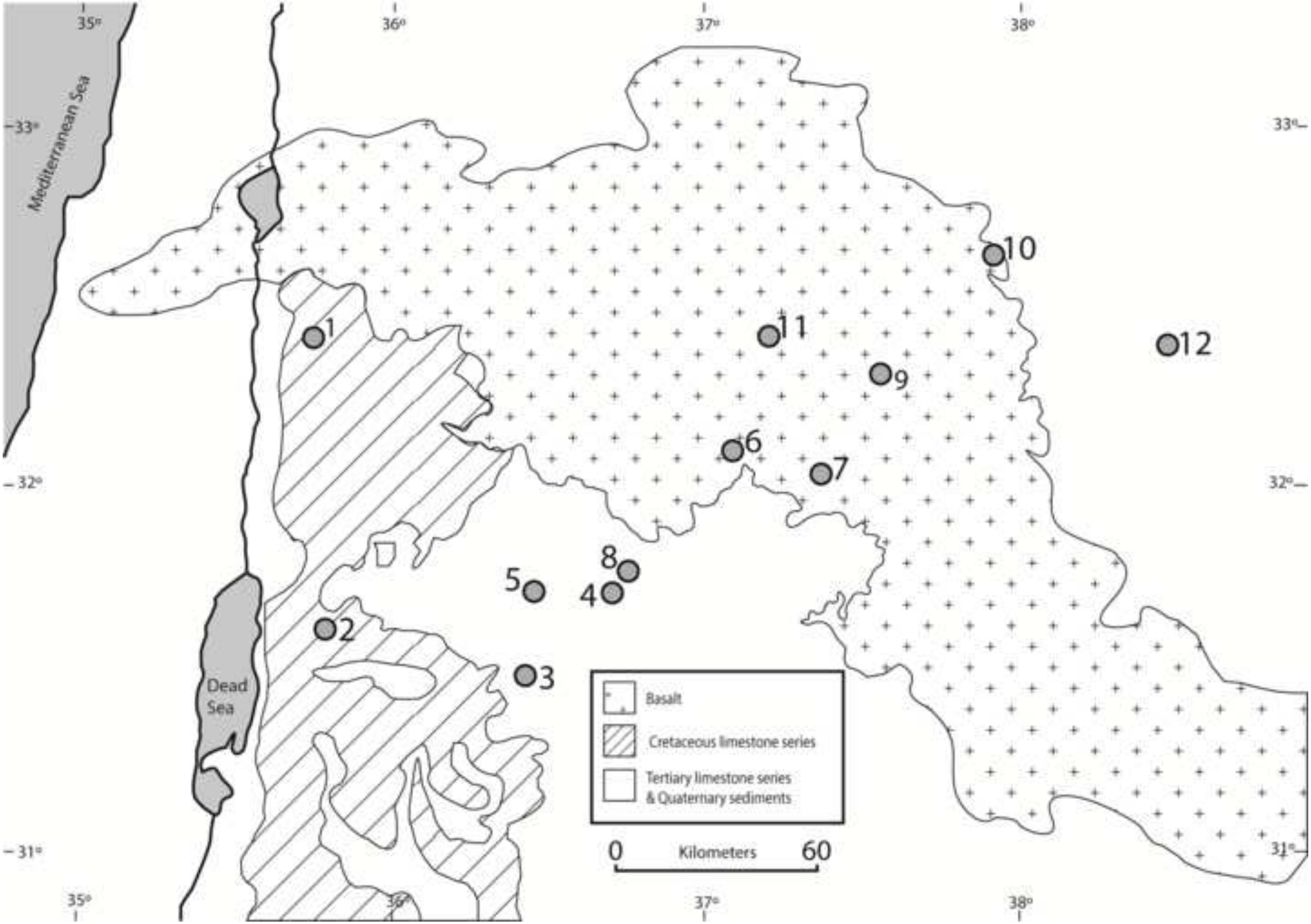

Fig 5. CARBON ISOTOPE GRAPH

Click here to download Non-colour figure Fig. 5 Carbon isotope graph.docx

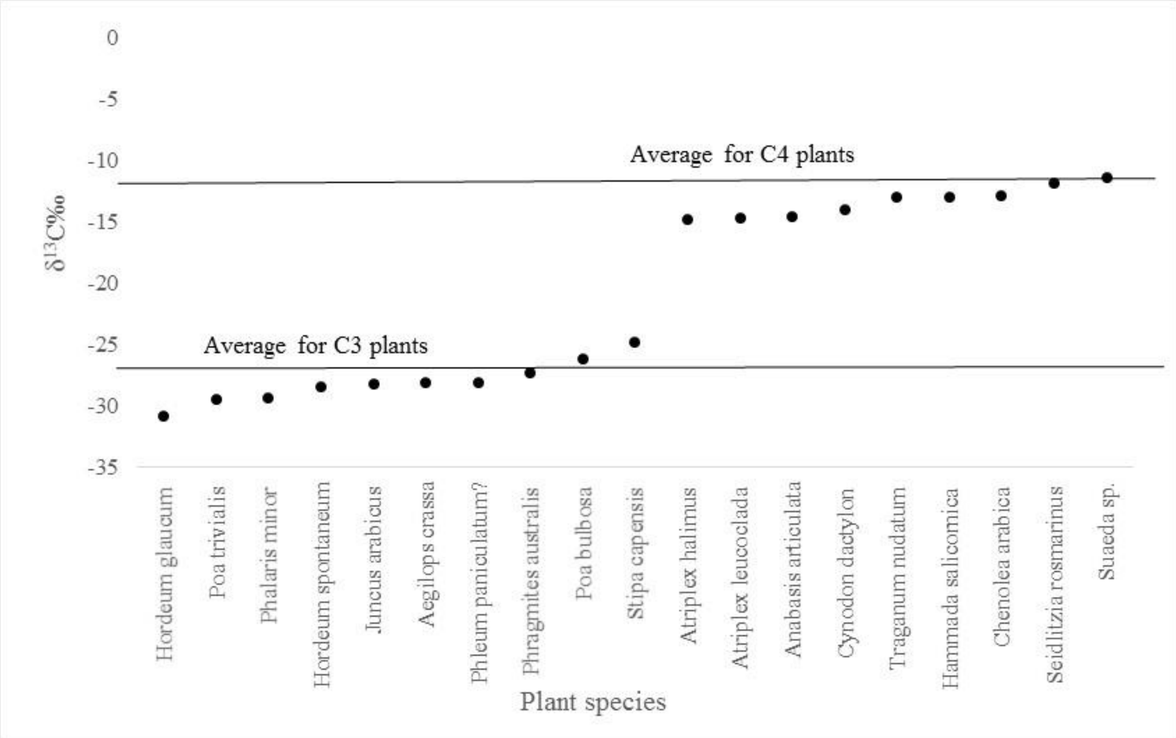

Fig 6. STRONTIUM ENDMEMBERS GRAPH

Click here to download Non-colour figure Fig. 6 strontium endmembers.docx

Fig 7. STRONTIUM MIXED SOURCES GRAPH

Click here to download Non-colour figure Fig. 7 strontium other points.docx

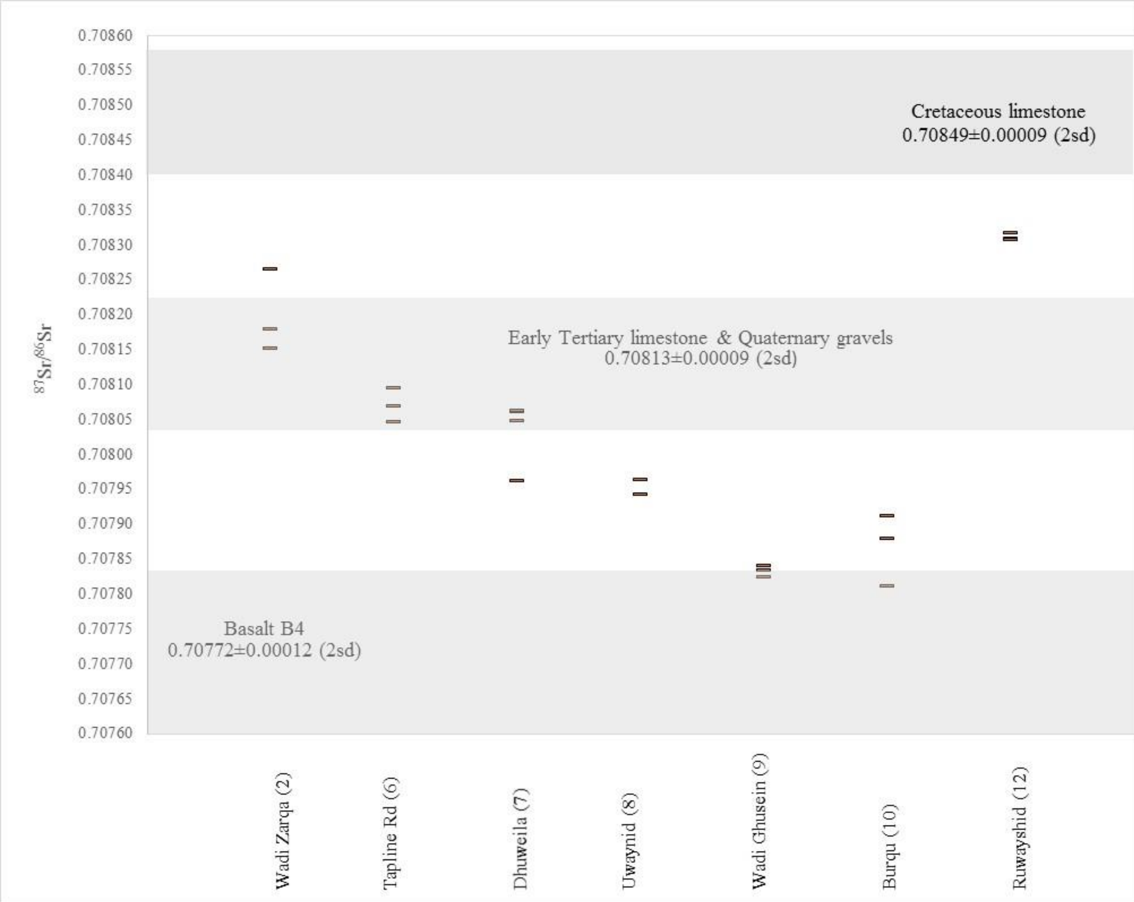

Fig 8. MOBILITY MODEL GRAPHS

Click here to download Non-colour figure Fig. 8 Model graphs.docx

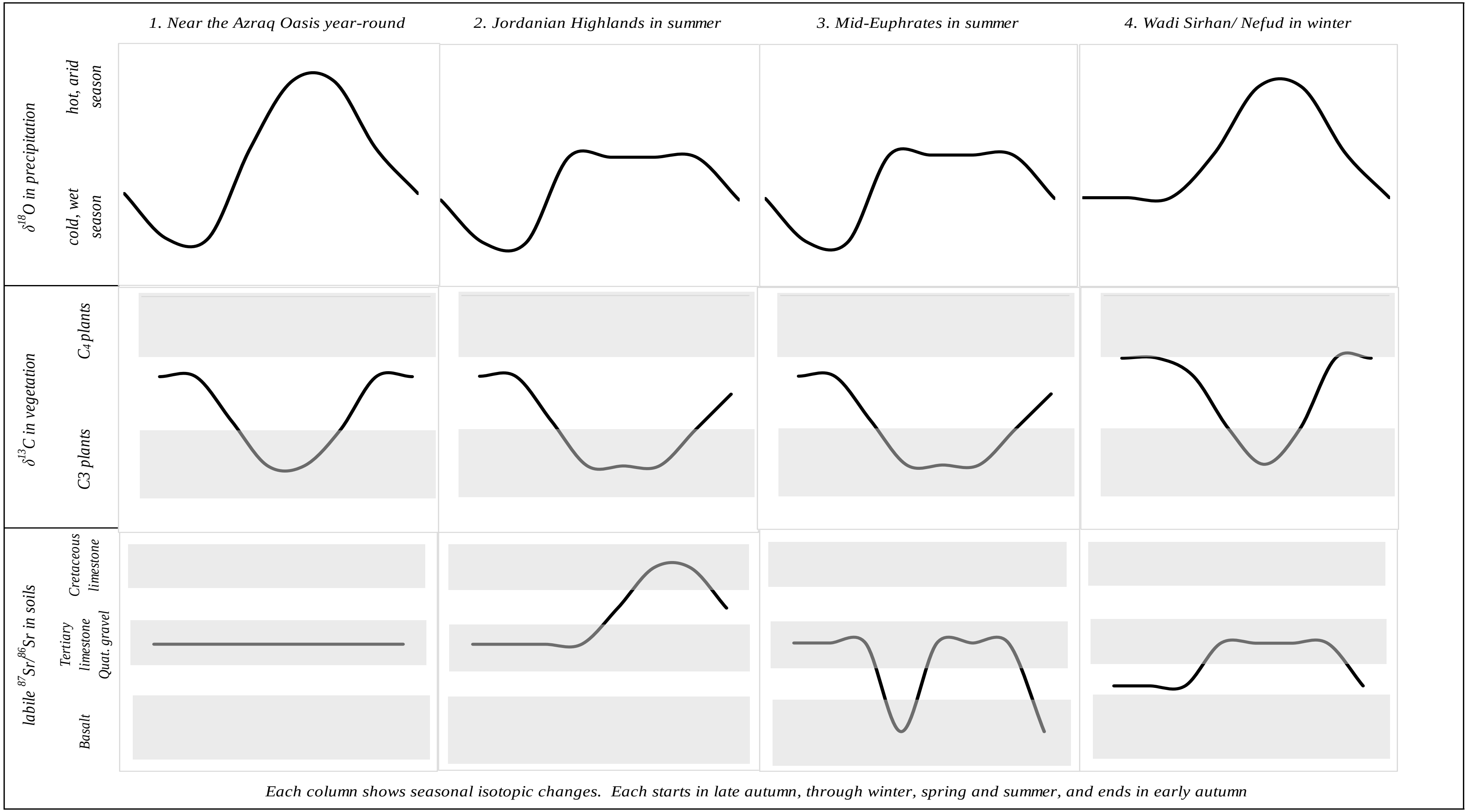

Supplementary 1. Details of modern plant collection locations

	Plant collection location	*UTM (Northern hemisphere)*	*Geological context*
1	Upper Wadi Yabis	$36.{}^{7}597$ E x ${}^{35}881$ N	Cretaceous limestone (c_2)
2	Upper Wadi Zarqa Ma'in	$36.{}^{7}576$ E x ${}^{35}002$ N	Cretaceous limestone (c_2)
3	Near Wadi Jilat 6	$37.{}^{2}546$ E x ${}^{34}884$ N	Eocene/Palaeocene limestones/marls (tt_1)
4	Shaumari Wildlife Reserve	$37.{}^{2}874$ E x ${}^{35}155$ N	Fluvial deposits draining from limestones/marls (tt_1)
5	Near Kharaneh IV	$37.{}^{2}587$ E x ${}^{35}128$ N	Fluvial deposits adjacent to limestones/marls (tt_1)
6	Tapline Road	$37.{}^{3}160$ E x ${}^{35}519$ N	Basalts (B_5)
7	Near Dhuweila	$37.{}^{3}443$ E x ${}^{35}457$ N	Basalts (B_4)
8	Near Uwaynid 14,18	$37.{}^{2}851$ E x ${}^{35}187$ N	Fluvial deposits adjacent to Basalts (B_5)
9	Wadi el Ghusein	$37.{}^{3}896$ E x ${}^{35}828$ N	Basalts (B_4)
10	Near Burqu	$37.{}^{4}026$ E x ${}^{36}085$ N	Basalts (B_4)
11	Shubayqa	$37.{}^{3}334$ E x ${}^{35}868$ N	Basalts (B_4)
12	Wadi Ruwayshid Salih	$37.{}^{4}441$ E x ${}^{35}993$ N	Eocene/Palaeocene limestones/marls (tt_1)

Supplementary 2. Photographs of all collected plant specimens

 *Achillea fragrantissima* (Forssk.) Sch. Bip.	 *Achillea santolina* L.	 *Aegilops crassa* Boiss.
 *Anabasis articulata* (Forssk.) Moq.	 Anthemis sp.	 *Artemisia herb-alba* Asso
 *Atriplex halimus* L.	 *Atriplex leucoclada* Boiss.	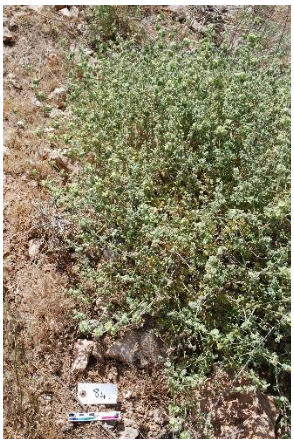 *Ballota undulata* (Sieber ex Fresen.) Benth.

 *Chenolea arabica* Boiss.	 *Cynodon dactylon* (L.) Pers.	 *Farsetia aegyptiaca* Turra
 *Gynandiris sisyrichium* (L.) Parl.	 *Hammada salicornica* (Moq.) Iljin	 *Hordeum glaucum* Steud.
 *Hordeum spontaneum* K. Koch	 *Juncus arabicus* (Asch. & Buchenau) Adamson	 *Malva parviflora* L.

 *Peganum harmala* L.	 *Phalaris minor* Retz.	 *Phleum paniculatum* Huds.?
 *Phlomis fruticosa* L.	 *Phragmites australis* Cav.) Trin. Ex Steud.	 *Poa bulbosa* L.
 *Poa trivialis* L.	 *Salvia heirosolymitana* Boiss	 *Seidlitzia rosmarinus* Bunge ex Boiss.

 *Stipa capenis* Thunb.	 Suaeda sp.	 *Teucrium polium* L.
 *Traganum nudatum* Delile	 *Trigonella stellata* Forssk.	

<table>
<tr><th rowspan="2">Specimen Number</th><th rowspan="2">Photo-grapher</th><th>Specimens</th><th>Collect ion</th><th colspan="9">Location</th></tr>
<tr><th>Taxa</th><th>Date & weather</th><th>Name</th><th>UTM (North Hemisphere)</th><th>m asl</th><th>Aspect</th><th>Soil (depth, structure, fertility)</th><th>Present wetness of soils</th><th>Hydrology (main water source)</th><th>Substrata</th><th>Vegetation association</th></tr>
<tr><td>12</td><td>IR</td><td>Poa trivialis L.</td><td>6.4.13 hot</td><td>Near Iraq ed Dubb (PPNA), Upper Wadi Yabis</td><td>36: 7.556 E x 35.845 N</td><td>917</td><td>Wadi bottom</td><td>Deep, arable soil</td><td>Very wet</td><td>Stream edge, near spring. 600 mm isohyet</td><td>Cretaceous C2. Limestone travertine</td><td>Deciduous oak</td></tr>
<tr><td>13</td><td>IR</td><td>Hammada salicornica (Moq.) Iljin</td><td rowspan="8">8.4.13 hot and very windy</td><td rowspan="8">Wadi Jilat
6 UP/EEP
7 E/MPPNB
8 MEP
9 UP
10 MEP
13 LN
22 MEP
25 LN
26 MPPNB
32 MPPNB</td><td rowspan="8">37: 2.546 E x 34.884N</td><td rowspan="8">785</td><td rowspan="2">Open, top</td><td rowspan="2">Thin, stony</td><td rowspan="2">Dry</td><td rowspan="8">Dry steppe. 100mm isohyet. Seasonal wadi and pools</td><td rowspan="8">Eocene/ Palaeocene (tt1). Limestone, cherts, marls, chalks, travertines</td><td rowspan="8">Limestone steppe</td></tr>
<tr><td>14</td><td>IR</td><td>Achillea fragrantissima (Forssk.) Sch. Bip.</td></tr>
<tr><td>17</td><td>IR</td><td>Hordeum glaucum Steud.</td><td rowspan="2">E-facing slope</td><td rowspan="2">Thin, stony</td><td rowspan="2">Dry</td></tr>
<tr><td>18</td><td>IR</td><td>Malva parviflora L.</td></tr>
<tr><td>20</td><td>IR</td><td>Atriplex leucoclada Boiss.</td><td rowspan="4">Wadi bottom</td><td rowspan="4">More alluvial, deeper,</td><td rowspan="4">Damp</td></tr>
<tr><td>21</td><td>IR</td><td>Suaeda sp.</td></tr>
<tr><td>22</td><td>IR</td><td>Chenolea arabica Boiss.</td></tr>
<tr><td>23</td><td>IR</td><td>Traganum nudatum Delile</td></tr>
</table>

24	LM	*Malva parviflora* L.	9.4.13 cool. Some cloud, little wind	Shubayqa 1 Natufian	37: 3.334 E x 35.868 N	740	Open, flat	Playa, relatively rich in silts, relatively fertile	Dry	Moist steppe. 150+ mm isohyet	Basalt B4 Lower Pleistocene/ Oligocene	Basalt steppe
25	LM	*Achillea fragrantissima* (Forssk.) Sch. Bip.										
26	IR	*Hordeum glaucum* Steud.										
28	LM	*Anabasis articulata* (Forssk.) Moq.										
30	IR	*Aegilops crassa* Boiss.		Wadi Salma	37: 3.379 E x 35.910 N	770	Small wadi bottom					
31	IR	*Phleum paniculatum Huds.?*										
32	IR	*Hordeum spontanaeum* K.Koch	10.4.13 cool, some cloud, little wind	Azraq - Shaumari Reserve	37: 2.874 E x 35.155 N	520	Ungrazed open steppe	Relatively good, due to veg cover.	Dry	Wadi-fed. 50+ mm isohyet	Pleistocene fluvial gravels and silts draining from Tertiary limestones	Calcareous Steppe
33	IR	*Seidlitzia rosmarinus* Bunge ex Boiss.										
34	LM	*Atriplex halimus* L.										
37	LM	*Stipa capenis* Thunb.										
38	IR	*Phalaris minor* Retz.										
40	IR	*Juncus arabicus* (Asch. & Buchenau Adamson		Azraq -Wetland	37: 2.937 E x 35.245 N	510	Wetland edge	Good soil cover, silt-rich	Wet 10 cm below surface.	Spring-fed		Wetland
41	IR	*Phragmites australis* (Cav.) Trin. Ex Steud.										

42	IR	*Achillea fragrantissima* (Forssk.) Sch. Bip.	11.4.13 cool. Some cloud, little wind	Dhuweila LPPNB, LN	37: 3.443 E x 35.457 N	640	Open, flat	Playa, rich in silts, relatively fertile	Wet 10 cm below surface.	Dry steppe. 50-100 mm isohyet. Seasonal wadi and occasional flooding.	Basalt B4 Lower Pleistocene/ Oligocene	Basalt steppe
45	IR	*Cynodon dactylon* (L.) Pers.										
46	IR	*Poa bulbosa* L.										
47	IR	*Trigonella stellata* Forssk.										
49	IR	*Stipa capenis* Thunb.										
51	IR	*Seidlitzia rosmarinus* Bunge ex Boiss.	12.4.13 warm, some cloud, little wind	Uwaynid 14 EEP 18 UP/EEP	37: 2.851 E x 35.187 N	525	Small wadi bottom	Accumulation of soils, silts, relatively deep	Soil wet 10 cm below surface.	Dry steppe. 50-100 mm isohyet. Seasonal wadi.	Basalt B5 Middle Pleistocene/ Miocene	Basalt steppe
52	LM	*Atriplex halimus* L.										
57	IR	*Hordeum glaucum* Steud.		Kharaneh IV EEP	37: 2.587 E x 35.128 N	640	Small wadi bottom	Poor, stony,	Dry	Dry steppe. 100 mm isohyet. Seasonal wadi flow	Pleistocene fluvial gravels and silts draining from Tertiary limestones	Limestone steppe
58	IR	*Achillea fragrantissima* (Forssk.) Sch. Bip.										
59	IR	*Malva parviflora* L.										
60	AG	*Phlomis fruticosa* L.	25.4.13 very warm, little wind	Upper Wadi Yabis	36: 7.597 E x 35.881 N	827	Naturally terraced NNE facing slope	Thin, stony, terra rossa	Dry	Rain-fed. 600 mm isohyet	Cretaceous C2. Limestone, chalk, marl, chert	Evergreen oak
61	AG	*Salvia heirosolymitana* Boiss.										
62	AG	Anthemis sp.										

64	AG	*Farsetia aegyptiaca* Turra	27.4.13 hot, very windy	Wadi Ruwayshid Salih (20 km east of Ruwayshid)	37: 4.441 E x 35.993 N	738	On flat, open desert	Thin, stony	Dry	Dry steppe. 50-100mm isohyet	Eocene/ Palaeocene (tt1). Limestone, cherts, marls, chalks	Limestone steppe
66	AG	*Gynandriris sisyrichium* (L.) Parl.										
67	IR	*Peganum harmala* L.										
74	IR	*Artemisia herb-alba* Asso	27.4.13	Wadi el Ghusein (74 km east of Safawi)	37: 3.896 E x 35.828 N	741	Small wadi bottom	Thin, stony	Dry	Dry steppe. 50-100 mm isohyet. Some seasonal wadi flow	Basalt B5 Middle Pleistocene/ Miocene	Basalt steppe
75	AG	*Farsetia aegyptiaca* Turra										
76	IR	*Achillea fragrantissima* (Forssk.) Sch. Bip.										
77	IR	*Achillea fragrantissima* (Forssk.) Sch. Bip.	27.4.13 cool, light breeze	Start of tapline road south of Safawi	37: 3.160 E x 35.519 N	688	Small wadi bottom	Thin, stony	Dry	Dry steppe. 50-100mm isohyet	Basalt B5 Middle Pleistocene/ Miocene	Basalt steppe
78	IR	*Euphorbia* sp.										
79	IR	*Artemisia herb-alba* Asso										
81	AG	*Teucrium polium* L.	1.5.13 hot, light breeze	Upper Wadi Zarqa Ma'in	36: 7.576 E x 35.002 N	714	North facing exposed sides of wadi	Thin, stony	Dry	Rain-fed. 300 mm isohyet	Cretaceous C2. Limestone, chalk, marl, chert	Park woodland
83	AG	*Achillea santolina* L.										
84	AG	*Ballota undulata* (Sieber ex Fresen.) Benth.										

Supplementary 4. Modern plant $\delta^{13}C$ and $^{87}Sr/^{86}Sr$ results. Details of published plant $\delta^{13}C$ data relevant to this research are included. See Fig. 4 for locations

Sample	*Taxa*	*Location (in vicinity, not on archaeological sites)*	$\delta^{13}C_{PDB}$	*Regionally relevant published* $\delta^{13}C_{PDB}$
12	*Poa trivialis*	Wadi Yabis	-29.4	
13	*Hammada salicornica*	Wadi Jilat	-12.9	-12.31
17	*Hordeum glaucum*	Wadi Jilat	-30.8	
20	*Atriplex leucoclada*	Wadi Jilat	-14.7	-15.6[1], -14[2], -13.56[4]
21	*Suaeda sp.*	Wadi Jilat	-11.4	-13.9 to -14.2[1], -11.5 to-13.6[2]
22	*Chenolea arabica*	Wadi Jilat	-12.9	-12.511
28	*Anabasis articulata*	Shubayqa	-14.6	-12.4[1], -11.70[3]
30	*Aegilops crassus*	Shubayqa	-28.1	
31	*Phleum paniculatum?*	Shubayqa	-28.1	
32	*Hordeum spontaneum*	Shubayqa	-28.5	
33	*Seidlitzia rosmarinus*	Shubayqa	-11.8	-12.6[1], -12.53[4]
34	*Atriplex halimus*	Shaumari	-14.8	-14.31
37	*Stipa capensis*	Shaumari	-24.8	
38	*Phalaris minor*	Shaumari	-29.3	
40	*Juncus arabicus*	Azraq wetland	-28.2	
41	*Phragmites australis*	Azraq wetland	-27.3	-25.45
45	*Cynodon dactylon*	Dhuweila	-14.0	-15.65
46	*Poa bulbosa*	Dhuweila	-26.1	
23	*Traganum nudatum*	Wadi Jilat	-13.0	-11.8[1], -12.9[2], -10.89[4]

[1]Shomer-Ilan et al 1981, [2]Winter 1981, [3]Ziegler et al 1981, [4]Akhani et al 1997, [5] Batanouny et al 1998

Sample	*Taxa*	*Location (in vicinity, not on archaeological sites)*	$^{87}Sr/^{86}Sr$	*Bedrock geology*
14.1	*Achillea fragrantissima*	3. Wadi Jilat 6,7	0.70807	Early Tertiary limestones (tt_1)
14.2	*Achillea fragrantissima*	3. Wadi Jilat 6,7	0.70808	Early Tertiary limestones (tt_1)
17.1	*Hordeum glaucum*	3. Wadi Jilat 6,7	0.70818	Early Tertiary limestones (tt_1)
17.2	*Hordeum glaucum*	3. Wadi Jilat 6,7	0.70818	Early Tertiary limestones (tt_1)
18.1	*Malva parviflora*	3. Wadi Jilat 6,7	0.70819	Early Tertiary limestones (tt_1)
18.2	*Malva parviflora*	3. Wadi Jilat 6,7	0.70818	Early Tertiary limestones (tt_1)
24.1	*Malva parviflora*	11. Shubayqa	0.70764	Basalt (B_4)
24.2	*Malva parviflora*	11. Shubayqa	0.70766	Basalt (B_4)
25.1	*Achillea fragrantissima*	11. Shubayqa	0.70773	Basalt (B_4)
25.2	*Achillea fragrantissima*	11. Shubayqa	0.70774	Basalt (B_4)
26.1	*Hordeum glaucum*	11. Shubayqa	0.70778	Basalt (B_4)
26.2	*Hordeum glaucum*	11. Shubayqa	0.70778	Basalt (B_4)
32	*Hordeum spontanaeum*	4. Shaumari Wildlife Reserve	0.70816	Fluvial deposits draining Early Tertiary limestones (tt_1)
34	*Atriplex halimus*	4. Shaumari Wildlife Reserve	0.70814	Fluvial deposits draining Early Tertiary limestones (tt_1)
37	*Stipa capensis*	4. Shaumari Wildlife Reserve	0.70812	Fluvial deposits draining Early Tertiary limestones (tt_1)
42	*Achillea fragrantissima*	7. Dhuweila	0.70806	Basalt (B_4)
47	*Trigonella stellata*	7. Dhuweila	0.70806	Basalt (B_4)
49	*Stipa capensis*	7. Dhuweila	0.70805	Basalt (B_4)
51	*Seidlitzia rosmarinus*	8. Uwaynid 14,18	0.70796	Fluvial deposits draiing Basalts (B_5)
52	*Atriplex halimus*	8. Uwaynid 14,18	0.70794	Fluvial deposits draining Basalts (B_5)
57	*Hordeum glaucum*	5. Kharaneh IV	0.70812	Fluvial deposits draining Early Tertiary limestones (tt_1)
58	*Achillea fragrantissima*	5. Kharaneh IV	0.70807	Fluvial deposits draining Early Tertiary limestones (tt_1)
59	*Malva parviflora*	5. Kharaneh IV	0.70808	Fluvial deposits draining Early Tertiary limestones (tt_1)
60	*Phlomis fruticosa*	1. Upper Wadi Yabis	0.70848	Cretaceous limestones (c_2)
61	*Salvia heirosolymitana*	1. Upper Wadi Yabis	0.70845	Cretaceous limestones (c_2)
62	Anthemis sp.	1. Upper Wadi Yabis	0.70854	Cretaceous limestones (c_2)
64	*Farsetia aegyptiaca*	12. Wadi Ruwayshid Salih, 20km E of Ruwayshid	0.70831	Early Tertiary limestones (tt_1)
66	*Gyandriris sisyrichium*	12. Wadi Ruwayshid Salih, 20km E of Ruwayshid	0.70831	Early Tertiary limestones (tt_1)
67	*Peganum harmala*	12. Wadi Ruwayshid Salih, 20km E of Ruwayshid	0.70831	Early Tertiary limestones (tt_1)
70	*Achillea fragrantissima*	10. Burqu	0.70781	Basalt (B_4)
71	*Malva parviflora*	10. Burqu	0.70788	Basalt (B_4)
72	*Atriplex leucoclada*	10. Burqu	0.70791	Basalt (B_4)
74	*Artemesia herb-alba*	9. Wadi el Ghusein, 74km E of Safawi	0.70783	Basalt (B_4)
75	*Farsetia aegyptiaca*	9. Wadi el Ghusein, 74km E of Safawi	0.70784	Basalt (B_4)
76	*Achillea fragrantissima*	9. Wadi el Ghusein, 74km E of Safawi	0.70783	Basalt (B_4)
77	*Achillea fragrantissima*	6. Tapline Road south of Safawi	0.70808	Basalt (B_5)
79	*Artemesia herb-alba*	6. Tapline Road south of Safawi	0.70810	Basalt (B_5)
80	*Peganum harmala*	6. Tapline Road south of Safawi	0.70805	Basalt (B_5)
81	*Teucrium polium*	2. Upper Wadi Zarqa Ma'in	0.70818	Cretaceous limestones (c_2)
83	*Achillea fragrantissima*	2. Upper Wadi Zarqa Ma'in	0.70827	Cretaceous limestones (c_2)
84	*Ballota undulata*	2. Upper Wadi Zarqa Ma'in	0.70816	Cretaceous limestones (c_2)